frontiers | Frontiers in Materials

TYPE Original Research
PUBLISHED 07 March 2024
DOI 10.3389/fmats.2023.1236266

OPEN ACCESS

EDITED BY
Bo-Tao Huang,
Zhejiang University, China

REVIEWED BY
Yu Xiang,
Hong Kong Polytechnic University, Hong Kong SAR, China
Trupti Ranjan Mahapatra,
Veer Surendra Sai University of Technology, India

*CORRESPONDENCE
Yasin Onuralp Özkılıç,
yozkilic@erbakan.edu.tr
Alireza Bahrami,
alireza.bahrami@hig.se
Alexey N. Beskopylny,
besk-an@yandex.ru

RECEIVED 07 June 2023
ACCEPTED 23 November 2023
PUBLISHED 07 March 2024

CITATION
Madenci E, Özkılıç YO, Bahrami A, Hakeem IY, Aksoylu C, Asyraf MRM, Beskopylny AN, Stel'makh SA, Shcherban' EM and Fayed S (2024), Behavior of functionally graded carbon nanotube reinforced composite sandwich beams with pultruded GFRP core under bending effect. *Front. Mater.* 10:1236266. doi: 10.3389/fmats.2023.1236266

Behavior of functionally graded carbon nanotube reinforced composite sandwich beams with pultruded GFRP core under bending effect

Emrah Madenci[1], Yasin Onuralp Özkılıç[1,2,3]*, Alireza Bahrami[4]*, Ibrahim Y. Hakeem[5], Ceyhun Aksoylu[6], Muhammad Rizal Muhammad Asyraf[7], Alexey N. Beskopylny[8]*, Sergey A. Stel'makh[9], Evgenii M. Shcherban'[10] and Sabry Fayed[11]

[1]Department of Civil Engineering, Necmettin Erbakan University, Konya, Türkiye, [2]Department of Civil Engineering, Lebanese American University, Byblos, Lebanon, [3]World Class Research Center, Advanced Digital Technologies, State Marine Technical University, Saint Petersburg, Russia, [4]Department of Building Engineering, Energy Systems and Sustainability Science, Faculty of Engineering and Sustainable Development, University of Gävle, Gävle, Sweden, [5]Department of Civil Engineering, College of Engineering, Najran University, Najran, Saudi Arabia, [6]Department of Civil Engineering, Konya Technical University, Konya, Türkiye, [7]Engineering Design Research Group, Faculty of Mechanical Engineering, Universiti Teknologi Malaysia, Johor Bahru, Johor, Malaysia, [8]Department of Transport Systems, Faculty of Roads and Transport Systems, Don State Technical University, Rostov-on-Don, Russia, [9]Department of Unique Buildings and Constructions Engineering, Don State Technical University, Rostov-on-Don, Russia, [10]Department of Engineering Geology, Bases, and Foundations, Don State Technical University, Rostov-on-Don, Russia, [11]Civil Engineering Department, Faculty of Engineering, Kafrelsheikh University, Kafr El Sheikh, Egypt

A novel generation of composite sandwich beams with laminated carbon fiber-reinforced polymer skins and pultruded glass fiber-reinforced polymer core materials was examined for their flexural behavior. The strength and failure mechanisms of the composite sandwich beams in flatwise and edgewise configurations were investigated using three-point static bending tests. These sophisticated composite structures must be designed and used in a variety of sectors, and our research provides vital insights into their performance and failure patterns. In comparison to the reference specimens (FGM-1), the carbon nanotube-reinforced specimens' bending capacity was affected and ranged from −2.5% to 7.75%. The amount of the carbon nanotube addition had a substantial impact on the beams' application level and load-carrying capacity. Particularly, the application of 0.5 wt% additive in the outermost fiber region of the beams, such as in FGM-4, led to an increase in the bending capacity. However, the stiffness values at the maximum load were decreased by 0.3%–18.6% compared to FGM-1, with the minimum level of the decrease in FGM-4. The experimental results were compared with the theoretical calculations based on the high-order shear deformation theory, which yielded an approximation between 11.99% and 12.98% by applying the Navier's solution.

KEYWORDS

composite sandwich beam, carbon nanotube, glass fiber-reinforced polymer, carbon fiber-reinforced polymer, flexural behavior, strength, bending capacity, stiffness

1 Introduction

In the past decade, composite structures have gained popularity in various industries, such as transportation, aviation, military, naval, and civil construction, owing to their remarkable characteristics (Wang et al., 2021; Li et al., 2022; Chen et al., 2023; Su et al., 2023; Zhang et al., 2023). Composite materials possess several advantageous features, such as their low weight, exceptional stiffness-to-weight ratio for bending, impressive fatigue resistance, superior thermal and damping properties, and high noise absorption capabilities (Karam and Tabbara, 2020; Sehar et al., 2022; Faddoul et al., 2023; Miniappan et al., 2023; Prasanthi et al., 2023; Sharma et al., 2023; Hakeem et al., 2024). Different types of composite materials have been utilized in civil engineering applications (Çelik et al., 2023; Fayed et al., 2023; Gerges et al., 2023; Tabbara and Karam 2020). Consequently, sandwich structures have emerged as a highly appealing option for a broad range of applications, underscoring the importance of continued research and development efforts to fully realize their potential (Garg et al., 2021; Ahmad et al., 2022a; Allehyani et al., 2022; Al-Muntaser et al., 2022; Ahmad et al., 2022b). Fiber composite sandwich elements have demonstrated to be a cost-effective and successful solution in civil infrastructures (Reddy, 2004; Vedernikov et al., 2020; Vedernikov et al., 2021; Huang et al., 2022; Sun et al., 2023). A typical sandwich structure consists of two thin layers of hard surface and a core bonded between them. A distinctive type of laminated composite, known as a sandwich structure, is created by bonding two thin yet rigid skins to a thick yet lightweight core. The core is typically made of hard materials such as metal or soft materials such as foam (Dawood et al., 2010). Incorporating sandwich structures in structural components provides a range of benefits, including significant increases in the bending stiffness and noteworthy improvements in strength-to-weight ratios. Reis and Rizkalla (2008) established the fundamental material properties of glass fiber-reinforced polymer (GFRP) composite sandwiches, including their behavior under flat compression and unidirectional bending, as well as skin tension and core shear.

Despite the advantages of using these materials, there may be certain limitations in their structural integrity, making them susceptible to a range of failure modes. One primary concern is the considerable deflection of sandwich beams due to their currently low Young's modulus, particularly when subjected to out-of-plane bending loads. The bending strength, rigidity, and energy absorption capacity of sandwich beams have been the subject of extensive research. The possible failure mechanisms for these structures include separation of the outer layers from the core material, buckling or wrinkling of the compression skin, core failure due to shear forces, crushing or penetration of the core owing to compression, tearing of the tension skin, and overall panel buckling. Ongoing research is crucial in improving the performance and reliability of sandwich beams, as emphasized by these challenges.

The dissociation of matrix-fiber linkages, matrix cracking, and other delamination phenomena are observed in sandwich structures and laminated composites. Functionally graded materials (FGMs) were created in response to these issues as a novel class of composites. By employing FGMs, the issue of tension-diverting effects and stress stripping effects that are seen in laminates may be avoided. Carrera et al. (2011), Elishakoff et al. (2015), and Chakraverty and Pradhan (2016) have authored books on functionally graded beams and plates. In a comprehensive survey, Sayyad and Ghugal (2019) undertook an in-depth analysis of sandwich beams made of FGMs. Their work presents a valuable contribution to the understanding and evaluation of these structures in various applications.

Nanomaterials have gained interest in different types of engineering applications (Mydin et al., 2023; Sathish et al., 2023; Suresh et al., 2023; Gul et al., 2023; Li et al., 2023). Due to their exceptional properties, carbon nanotubes (CNTs) have recently found extensive use in polymer-based nanocomposites (Said et al., 2023a; Prasanthi et al., 2023; Gul et al., 2023; Devi et al., 2023; Said et al., 2023b). Experimental studies have shown that CNTs possess superior mechanical characteristics in comparison to continuous carbon fibers (Sun et al., 2005; Jia et al., 2011; Ahmad et al., 2022c). The incorporation of single- or multi-walled CNTs (SWCNTs or MWCNTs) in polymer films can greatly enhance their mechanical properties, including the tensile modulus, yield strength, and ultimate strength. Aligned CNTs noticeably improve the strength of reinforced films, in contrast to randomly oriented nanotubes (Benbakhti et al., 2016; Thai et al., 2018). Consequently, the development of functionally graded composite structures reinforced with nanoparticles has recently gained momentum thanks to their low weight and potential applications in various fields. The potential applications of such structures are diverse, ranging from micro-sensors, orthopedic implants, and biomedical instruments to aerospace and automotive engineering, shipbuilding, lightweight armor materials, and nuclear power plants (Shen, 2009; Thai et al., 2018). Experimental measurements of elastic modulus in composites containing CNTs have indicated an increase in the modulus compared to the pristine matrix (Schadler et al., 1998; Qian et al., 2002; Zhu et al., 2004; Barretta et al., 2015).

Gojny et al. (2005) examined the effects of incorporating single-, double-, and multi-walled CNTs on the mechanical properties of epoxy-based nanocomposites. Their findings illustrated that amino-functionalized double-walled CNTs at a filler content of 0.5 wt% resulted in the most remarkable improvements, including a 10% increase in the tensile strength, a 15% increase in the stiffness, and a 43% increase in the fracture toughness. Tarfaoui et al. (2016) evaluated the mechanical behavior of textile composites reinforced with CNTs and their effects on elastic properties. Specimens with volume fractions, varying from 0% to 4%, were prepared. The authors used open hole tension, shear bear tension, and flatwise tension tests for the assessment of the elastic modulus of textile composites with and without CNTs. Demircan et al. (2020) utilized commingled yarns (low melting point polyethylene terephthalate fiber/glass fiber) and a hot-press machine to produce thermoplastic composites with four different weight percentages of MWCNTs (0.0, 0.7, 0.9, and 1.1 wt%). The results indicated that the chemical bonding of CNTs to glass fibers led to a slight reduction in the tensile strength of nanocomposites, but an increase in their flexural strength.

Agglomeration in CNT-reinforced composites is a problem caused by the bending, curling, or agglomeration tendency of CNTs. Agglomeration can reduce the mechanical properties of the composite and negatively affect its performance (García-Macías et al., 2018; Bisheh et al., 2020). The following methods and measures can be employed to solve this problem. Proper dispersion: It is essential to ensure that CNTs are uniformly dispersed within the composite matrix. Suitable dispersion methods and chemical dispersants can be used to prevent the nanotubes from sticking together. This helps achieve a homogeneous distribution of the nanotubes. Matrix selection: The choice of the polymer matrix in the composite should be compatible with CNTs and designed to reduce agglomeration tendencies. A matrix material with high viscosity and suitable interaction with CNTs can minimize agglomeration. Ultrasonic

treatment: Ultrasonic treatment can aid in the homogeneous dispersion of nanotubes within the matrix. The energy from ultrasonic waves weakens the bonds between the nanotubes, preventing agglomeration. Surface modification: Chemical modifications of CNT surfaces can improve their compatibility with the matrix, reducing their tendency to stick together. High-temperature processing: Utilizing high-temperature processes during composite fabrication can enhance the integration of nanotubes with the matrix and reduce agglomeration. Lower tube concentration: Reducing the concentration of CNTs can alleviate the agglomeration problem. Lower concentrations result in reduced agglomeration tendencies. Mold filling: Ensuring proper filling of the composite material during the molding process can facilitate a more uniform distribution of the nanotubes. Continuous production techniques: Continuous production techniques can decrease agglomeration in high-volume composite manufacturing. These techniques provide better control over dispersion (Pan et al., 2016; Tornabene et al., 2016).

FGMs have continuously varying volume ratios of their components, with ratios that shift across the thickness of the structure (Madenci, 2019; Madenci, 2023). Another important aspect of constructing polymer structures is the incorporation of the CNT reinforcement. An important issue in fiber-reinforced polymer (FRP) composites is the reinforcement of the interlayer region. The properties of the regions between weak layers limit the overall performance of laminated FRP composite structures. In FGMs, the change of material properties has a functional transition. Therefore, there is no delamination problem (Uyaner and Yar, 2019). The optimum feasible utilization (spread) of a given amount of reinforcement in polymer specimens is essential considering the high cost of CNTs. Functionally graded CNT reinforced composites (FG-CNTRCs) are a unique class of materials that feature a constant distribution of CNT reinforcements and are made possible by the linear arrangement of CNTs within a matrix. The use of the FGM concept and how the reinforcement behavior of FG-CNTRC plates in nonlinear bending analysis can be increased by the functionally graded distribution of CNTs were revealed with the potential benefits of utilizing FGMs in conjunction with CNTs to improve the properties of composite structures. Nonlinear vibration and bending of FG-CNTRCs were assessed by Kaci et al. (2012). Phung-Van et al. (2015) developed an efficient formulation employing iso-geometric analysis and higher-order shear deformation theory to investigate the static and dynamic behaviors of FG-CNTRCs. Madenci (2021) utilized variational formulations to perform a free vibration analysis on nanobeams made of FG-CNTRC, where the effective material properties of SWCNT-reinforced nanobeams were estimated using the rule of mixture. This research provided valuable insights into the dynamic behavior and performance of FG-CNTRC structures in different applications.

It is crucial to apply both the first-order shear deformation theory (Timoshenko theory) and higher-order shear deformation theories when dealing with structures such as sandwich beams with CNTRC face-sheets, as these structures exhibit a significant impact of the shear deformation (Viola et al., 2014; Payton et al., 2017; Draiche et al., 2019; Draoui et al., 2019; Hussain et al., 2019; Hellal et al., 2021). The nonlinear free vibration of temperature-dependent sandwich beams with CNTRC face-sheets was investigated by Mirzaei and Kiani (2016) using the Timoshenko beam theory and Ritz technique with polynomial basis functions. Applying a finite element approach based on the first-order shear deformation theory, static and free vibration analyses were carried out on nanocomposite plates reinforced with straight CNTs by Zhu et al. (2012). Mehar et al. (2016) proposed a finite element method based on the higher-order shear deformation theory to analyze the free vibration of FG-CNTRCs in a heated environment. The mentioned studies provided valuable insights into the intricate behavior of composite structures across different scenarios, emphasizing the need to consider shear deformation effects when analyzing such elements (Mehar et al., 2017; Mehar et al., 2018).

Unlike the research conducted on sandwich beams made of layered FG-CNTRCs, there is a scarcity of research on sandwich beams comprising of rigid cores and FG-CNTRC face-sheets. In this study, an examination of the bending behavior of structural composite sandwich beams with pultruded GFRP core material and laminated carbon fiber composite sheaths reinforced with CNTs is presented. Undergoing three-point static bending tests, the load-deflection behavior and damage analysis of the FG-CNTRC sandwich beams were evaluated, while their static behavior was theoretically predicted using the properties of the skin and core materials, acquired through coupon tests. By contrasting the experimental outcomes with the theoretical predictions, it was possible to gain more insight into the functionality of such composite structures, and hence, to underline the necessity for continued investigation in this domain.

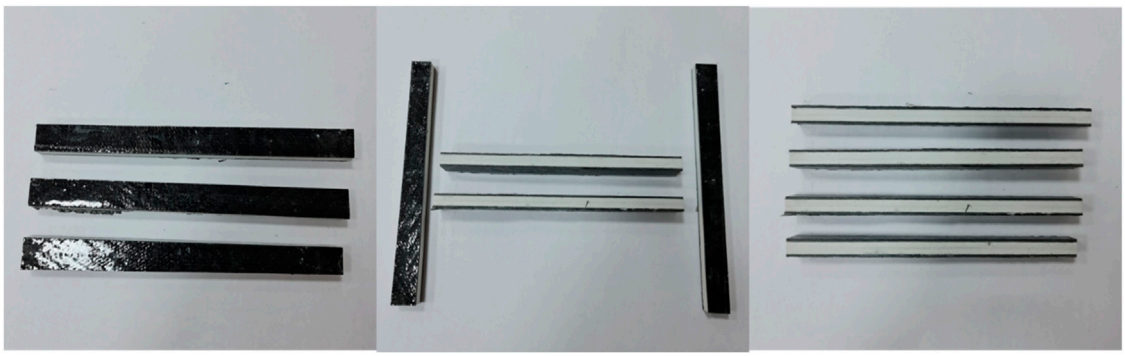

FIGURE 1
Test specimens.

TABLE 1 Design of specimens.

%0 CNT	%0.3 CNT	%0.5 CNT	%0.3 CNT	%0.5 CNT
%0 CNT	%0.4 CNT	%0.4 CNT	%0.4 CNT	%0.4 CNT
%0 CNT	%0.5 CNT	%0.3 CNT	%0.5 CNT	%0.3 CNT
Core	**Core**	**Core**	**Core**	**Core**
%0 CNT	%0.5 CNT	%0.3 CNT	%0.3 CNT	%0.5 CNT
%0 CNT	%0.4 CNT	%0.4 CNT	%0.4 CNT	%0.4 CNT
%0 CNT	%0.3 CNT	%0.5 CNT	%0.5 CNT	%0.3 CNT
FGM-1	**FGM-2**	**FGM-3**	**FGM-4**	**FGM-5**

2 Materials

2.1 Design of specimens

The sandwich beams examined in this study comprised composite coatings featuring a carbon fiber layer reinforced with CNTs. These coatings were applied onto a GFRP core material that had been produced via the pultrusion process (Figure 1). Pultruded GFRP materials were successfully utilized in engineering applications (Aksoylu et al., 2022; Madenci et al., 2022a; Özkılıç et al., 2022a; Madenci et al., 2022b; Özkılıç et al., 2022b; Vedernikov et al., 2022; Madenci et al., 2023).

Five functionally graded composites, each with a distinct configuration, were assessed during the three-point bending tests. Pultruded lamina was used as a core element for all specimens. Three layers of carbon FRP (CFRP) were bonded beneath the core element, while another three layers were bonded above it. The specimens' design is given in Table 1. The first specimen (FGM-1) did not include any CNTs in its CFRP layers. The second specimen (FGM-2) employed CNT ratios of 0.3%, 0.4%, and 0.5% from top to bottom for its CFRP layers. Symmetrical distribution was selected for the bottom part. The third specimen (FGM-3) utilized CNT ratios of 0.5%, 0.4%, and 0.3% from top to bottom for its CFRP layers. Symmetrical distribution was also selected for the bottom part. The fourth specimen (FGM-4) used CNT ratios of 0.3%, 0.4%, and 0.5% from top to bottom for its CFRP layers. Anti-symmetrical distribution was selected for the bottom part. The fifth and final specimen (FGM-5) utilized CNT ratios of 0.5%, 0.4%, and 0.3% from top to bottom for its CFRP layers, and anti-symmetrical distribution was selected for the bottom part. The thickness of each layer was 0.6 mm.

2.2 CNT reinforced CFRP sheets

Two-phase epoxy resin was used that comprises a combination of aliphatic diglycidyl ether (10%–20%) and diglycidyl ether bisphenol A (80%–90%). The resin has a viscosity range of 600–900 mPa·s. Table 2 lists the mechanical characteristics of epoxy resin in accordance with DIN WL 5.3203-11:1978-11 standard. This study selected MWCNTs over their single-walled counterparts due to their more even dispersion in epoxy resins and affordability. The mechanical properties of CNTs, which had a diameter ranging from 5 to 50 nm and a length between 10 and 30 m, are provided in Table 3. For this research, a plain weave 200 g carbon fiber cloth was produced using Tenax-E HTA 40 3 k yarn. Carbon fiber fabric is an ideal choice for applications that require a combination of lightweight, strength, and carbon properties. Table 4 presents the mechanical properties of the utilized CFRP material. Three layers of carbon fibers were combined with resin epoxy to produce the composite material.

The vacuum infusion was used to create composite plates containing an epoxy matrix and reinforced with carbon fiber, achieved by symmetrically layering three fabric layers onto a mold and injecting resin. The composite plates underwent a 24-h room temperature curing process. The same technique was applied to nanoparticles made of three layers of carbon fiber fabric. At this stage, the epoxy matrix had been infused with MWCNTs at weight percentages of 0.3, 0.4, and 0.5. The epoxy resin and CNT powder were mixed during the initial phase using a mechanical stirrer for 15 min. After using a mechanical stirrer in the initial phase, ultrasonic homogeneity equipment was employed. Bandelin Electronics UW2200 model ultrasonic mixer device was used. The dispersion process was carried out with an ultrasonic homogenizer device at a power rate of 15%

TABLE 2 Mechanical properties of epoxy resin.

Tensile strength (MPa)	Young's modulus (kPa)	Elongation at break (%)	Density (g/cm^3)
70-80	3-3.3	5-6.5	1.18-1.20

TABLE 3 Mechanical properties of CNTs.

Tensile strength (GPa)	Young's modulus (TPa)	Elongation at break (%)	Density (g/cm^3)
10-60	1	1.3-2	10

TABLE 4 Mechanical properties of CFRP.

Tensile strength (MPa)	Young's modulus (GPa)	Elongation at break (%)	Density (g/cm^3)
3,950	238	1.7	1.76

and for 15 min. A vacuum infusion process was utilized to inject the resin reinforced with nanoparticles into the carbon fiber fabric (Figure 2).

2.3 Pultruded GFRP core

The low strength values of building elements made of composite materials due to production methods such as fiber wrapping and resin transfer molding limit their resistance to incoming loads. In response, researchers have been searching for innovative manufacturing methods. One such method is the pultrusion process, which enables the production of profile elements with high strength values, simple mass manufacturing, and low cost. In the pultrusion technique, continuous fibers are the preferred reinforcement material and can be employed in woven or broken felts and roving. The matrix material is typically polyester. The pultruded GFRP composite was used in the sandwich beam's core for this study. The longitudinal and transverse directions have elastic modulus of 21 GPa and 6 GPa, respectively. Meanwhile, the longitudinal and transverse directions have tensile strengths of 320 MPa and 80 MPa, respectively.

3 Experimental test

Experimental studies on FG-CNTRC sandwich beams were performed. The hybrid beams were subjected to three-point loading conditions with a 1 kN/min loading speed. The specimens had a length of 250 mm and a span length of 200 mm, and were tested using the setup illustrated in Figure 3.

4 Theory and formulation

It is well known that similar single-layer theories cannot accurately describe sandwich architectures when the core layer is not rigid. In contrast, a sandwich beam with a rigid core can be effectively formulated using an analogous single-layer theory. Due to the stiff material of the host layer in this study, the kinematics of the beam can be estimated using an analogous single-layer theory. However, to develop the sandwich beam with FG-CNTRC faces, the higher-order shear deformation beam theory was utilized in the current study. The displacement model of the FG-CNTRC sandwich beam, as per the higher-order shear deformation theory, can be expressed as:

$$\begin{aligned} u(x,z,t) &= u_0(x,t) - z\frac{\partial w_b}{\partial x} - f(z)\frac{\partial w_s}{\partial x} \\ w(x,z,t) &= w_b(x,t) + w_s(x,t) \end{aligned} \tag{1}$$

By applying the following equations, one can derive the kinematic relations:

$$\begin{aligned} \varepsilon_x &= \frac{\partial u_0}{\partial x} - z\left(\frac{\partial^2 w_b}{\partial x^2}\right) - f(z)\left(\frac{\partial^2 w_s}{\partial x^2}\right) \\ \gamma_{xz} &= \left(1 - f'(z)\right)\frac{\partial w_s}{\partial x} \end{aligned} \tag{2}$$

When there is a temperature variation, the constitutive equations of the beam, which are limited to the axial and transverse stress components, can be represented as follows:

$$\begin{aligned} \sigma_x &= Q_{11}(z)\varepsilon_x \\ \tau_{xz} &= Q_{55}(z)\gamma_{xz} \end{aligned} \tag{3}$$

The material constants are used to evaluate Q_{11} and Q_{55}, as shown in the equations below:

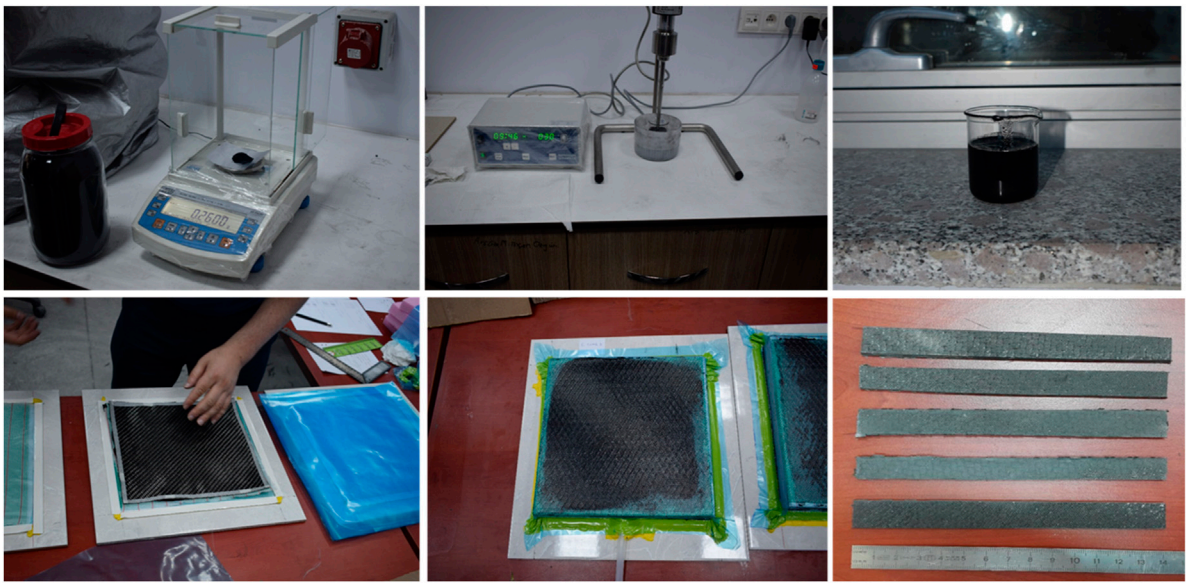

FIGURE 2
FG-CNTRC plates manufacturing.

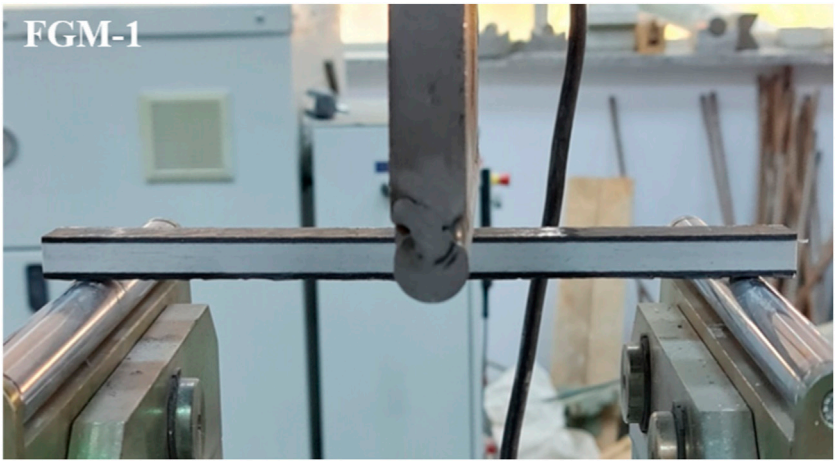

FIGURE 3
Setup of three-point bending test.

$$\begin{aligned} Q_{11} &= E_{11} \\ Q_{55} &= G_{13} \end{aligned} \tag{4}$$

By applying the principle of virtual displacements, one can derive the governing equations of equilibrium. In this scenario, the principle of virtual work produces the following result:

$$\int_{-h/2}^{h/2}\int_{0}^{L}[\sigma_x\delta\varepsilon_x+\tau_{xz}\delta\gamma_{xz}]dxdz-\int_{0}^{L}F(L/2)(\delta w)dx=0 \tag{5}$$

By integrating Eq. 5 throughout the beam's thickness and substituting Eqs. 2, 3 into it, the resulting equation can be expressed as:

$$\begin{aligned} &\int_{0}^{L}\left(N_x\frac{d\delta u_0}{dx}-M_x^b\frac{d^2\delta w_b}{dx^2}-M_x^s\frac{d^2\delta w_s}{dx^2}+Q_{xz}\frac{d\delta w_s}{dx}\right)dx \\ &-\int_{0}^{L}F(\delta w_b+\delta w_s)dx=0 \end{aligned} \tag{6}$$

Eq. 6 defines the stress resultants as:

$$\begin{aligned} (N_x,M_x^b,M_x^s) &= \sum_{n=1}^{3}\int_{-h/2}^{h/2}(1,z,f(z))\sigma_x dz \\ Q_{xz} &= \sum_{n=1}^{3}\int_{-h/2}^{h/2}(1-f'(z))\tau_{xz}dz \end{aligned} \tag{7}$$

By setting the coefficients where δu_0, δw_b, δw_s are zero and integrating the displacement gradients by parts, the governing equations of the equilibrium can be derived from Eq. 6. As a result, the equilibrium equations for the higher-order shear deformation beam theory can be derived as follows:

$$\begin{aligned} \delta u_0&: \frac{dN_x}{dx}=0 \\ \delta w_b&: \frac{d^2M_x^b}{dx^2}+F=0 \\ \delta w_s&: \frac{d^2M_x^s}{dx^2}+\frac{dQ_{xz}}{dx}+F=0 \end{aligned} \tag{8}$$

Expressing Eq. 8 in terms of displacements yields the equations below:

$$\begin{aligned} A_{11}\frac{\partial^2u_0}{\partial x^2}-B_{11}\frac{\partial^3w_b}{\partial x^3}-B_{11}^s\frac{\partial^3w_s}{\partial x^3}&=0 \\ B_{11}\frac{\partial^3u_0}{\partial x^3}-D_{11}\frac{\partial^4w_b}{\partial x^4}-D_{11}^s\frac{\partial^4w_s}{\partial x^4}+F&=0 \\ B_{11}^s\frac{\partial^3u_0}{\partial x^3}-D_{11}^s\frac{\partial^4w_b}{\partial x^4}-H_{11}^s\frac{\partial^4w_s}{\partial x^4}+A_{55}^s\frac{\partial^2w_s}{\partial x^2}+F&=0 \end{aligned} \tag{9}$$

where the beam stiffness is defined by:

$$\begin{aligned} (A_{11},B_{11},D_{11},B_{11}^s,D_{11}^s,H_{11}^s) &= \sum_{n=1}^{3}\int_{-h/2}^{h/2}Q_{11}(1,z,z^2,f(z),zf(z),f^2(z))dz \\ A_{55}^s &= \sum_{n=1}^{3}\int_{-h/2}^{h/2}Q_{55}[1-f'(z)]^2dz \end{aligned} \tag{10}$$

The Navier's solution technique can be utilized to obtain closed-form solutions for FG-CNTRC sandwich beams that are simply supported and subjected to a point load f. This method provides a detailed insight into the behavior and performance of the beam under particular loading scenarios.

$$\begin{aligned} u_0 &= \sum_{m=1}^{\infty}U_m\cos(\lambda x) \\ w_b &= \sum_{m=1}^{\infty}W_{bm}\sin(\lambda x) \\ w_s &= \sum_{m=1}^{\infty}W_{sm}\sin(\lambda x) \end{aligned} \tag{11}$$

10.3389/fmats.2024.1236266

TABLE 5 Experimental and analytical bending test results.

Results	FGM-1	FGM-2	FGM-3	FGM-4	FGM-5
Maximum load (kN)	4.00	4.06	4.23	4.31	3.90
Increase rate (%)	1	1.5	5.7	7.7	−2.5
Experimental displacement (mm)	14.59	15.89	18.40	15.78	17.42
Increase rate (%)	1	8.9	26.1	8.1	19.3
Theoretical displacement (mm)	16.34	17.87	20.79	17.80	19.61
Increase rate (%)	1	9.3	27.2	8.9	20.0

Arbitrary parameters U_m, W_{bm}, and W_{sm} can be determined in the following equation to obtain analytical solutions, while $\lambda = m\pi/L$.

$$\begin{bmatrix} A_{11}\lambda^2 & -B_{11}\lambda^3 & -B^s_{11}\lambda^3 \\ -B_{11}\lambda^3 & D_{11}\lambda^4 & D^s_{11}\lambda^4 \\ -B^s_{11}\lambda^3 & D^s_{11}\lambda^4 & H^s_{11}\lambda^4 + A^s_{55}\lambda^2 \end{bmatrix} \begin{Bmatrix} U_m \\ W_{bm} \\ W_{sm} \end{Bmatrix} = \begin{Bmatrix} 0 \\ F \\ F \end{Bmatrix} \quad (12)$$

5 Results

Table 5 displays the experimental and theoretical displacement outcomes, while Figure 4 depicts the load-displacement curves. Based on the load-displacement findings in Table 5, the FGM-4 specimen had the greatest load-carrying capacity, while the FGM-3 specimen exhibited the highest displacement. The addition of CNTs resulted in a slight improvement in the load-carrying capacity. The experimental and theoretical outcomes were consistent with each other, demonstrating that the introduction of CNTs enhanced the beams' behavior in terms of the load-carrying capacity and stiffness, irrespective of the FGM composition. In comparison to FGM-1, FGM-2, FGM-3, and FGM-4 showed a 1.5%, 5.7%, and 7.75% increase in the load-carrying capacity, respectively, while FGM-5 revealed a 2.5% decrease. However, at maximum load, FGM-1 had a stiffness of 0.274 kN/mm, while FGM-2, FGM-3, FGM-4, and FGM-5 had 6.9%, 16.4%, 0.3%, and 18.6% less stiffness vlaues, respectively. These results indicated the importance of the CNT ratio and location. The average bending capacity of FGM-1, FGM-2, FGM-3, FGM-4, and FGM-5 specimens was recorded at 4, 4.06, 4.23, 4.31, and 3.90 kN, respectively. The FGM-4 combination gave the most noticeable improvement in the capacity, with a 7.75% increase compared to the baseline specimen FGM-1. The maximum load values taken from Figure 4 were used in the bending equations and the collapse values were obtained theoretically. It was observed that the obtained displacement results and the experimental displacement results corresponding to the same load values were close to each other.

6 Damage analysis

Macroscopic damage analyses were conducted based on the load-displacement curves and observations made during the experiments. Figure 5 presents the representative load-

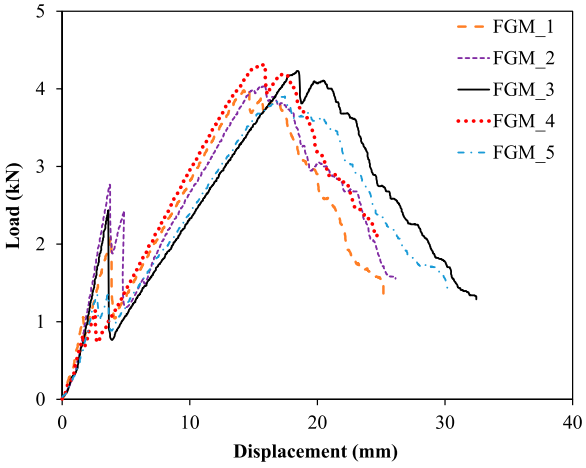

FIGURE 4
Load-displacement curves of tested specimens.

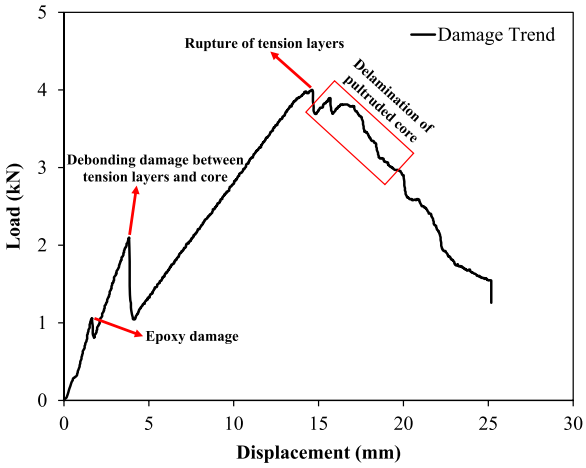

FIGURE 5
General damage behavior according to the load-displacement curve.

10.3389/fmats.2024.1236266

displacement curves with damage trend behavior for all experimental specimens. The experiment was terminated in four stages for all specimens. The first damage with the applied load occurred in the epoxy that provides the interlayer connection. This moment was the phase where the first interface separation was stimulated for the specimens and the first peak was ensured to occur. As the load increased, the debonding damage between the tension layer and core occurred, and the load value decreased a little. After this stage, a considerable increase in the load occurred, and the maximum load level was reached. A rupture of the tension layer was observed at this moment when the tensile stresses were maximum. Finally, the experiment ended with a slight increase and decrease in the load and delamination of the pultruded core.

In three-point bending, it is common to observe different types of failure modes, as illustrated in Figure 6. The results obtained from the experiments carried out on FGM-1 and FGM-2 indicated that the initial damage in longitudinal specimens occurred in the form of crushing at their mid-span middle surface. As the load increased, delamination also occurred, leading to the final failure of the specimens. The failure mechanism witnessed in the FGM-3, FGM-4, and FGM-5 specimens involved the initiation of transverse fractures on the lower surface of the specimens, followed by debonding of the upper surface at increased loads, culminating in the final failure.

According to the experimental findings, the longitudinal specimens displayed instances of the delamination and debonding. Figure 7 demonstrates visible cracks that emerged at the junction between the pultruded roving and CFRP laminates. Based on this observation, it can be inferred that the key factor contributing to the deterioration of mechanical properties in longitudinal specimens is weakening of the bond between the pultruded roving and laminates at their interface. Understanding this failure mechanism is crucial for improving the design and

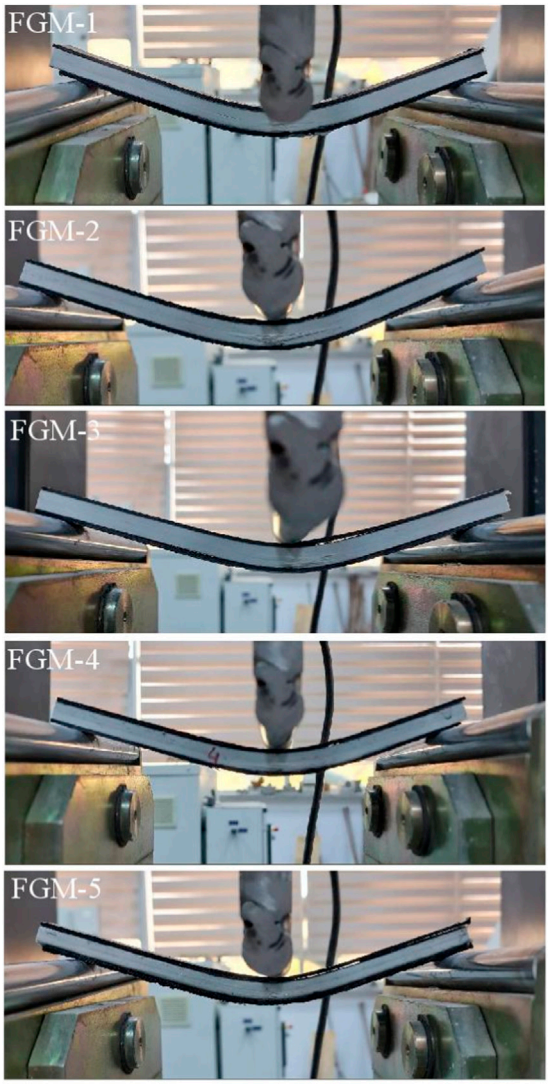

FIGURE 6
Typical failure modes of specimens tested in flexure.

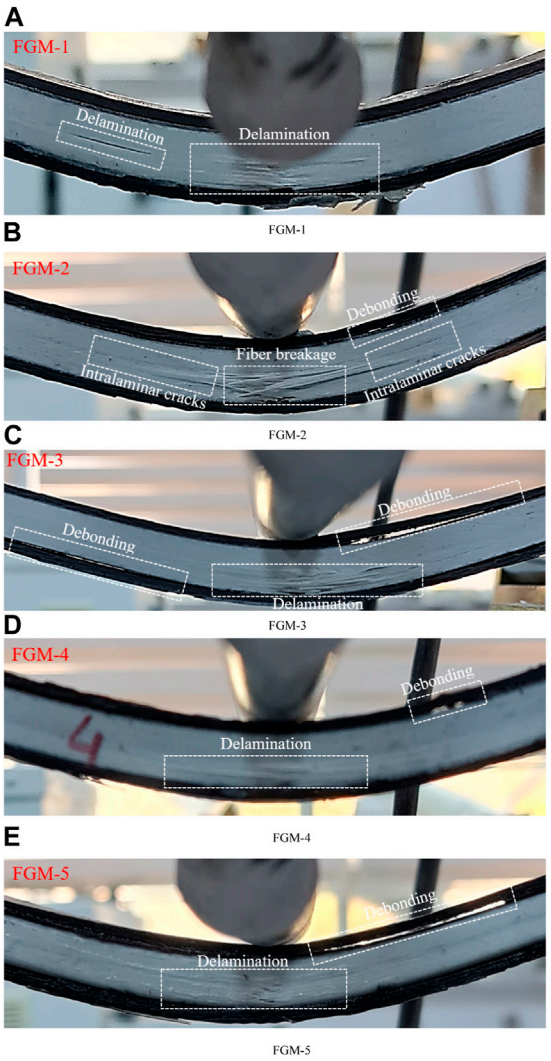

FIGURE 7
Typical failure mechanisms of bending specimens at different CNT ratios.

performance of FG-CNTRC sandwich beams in various applications.

7 Conclusions

In this study, sandwich beams, the lower and upper surfaces of which were composed of carbon fiber layers containing CNT at different rates, and the core of pultruded GFRP composites, were subjected to bending. Their behavior was investigated experimentally and theoretically, and the damage development was evaluated by the damage analysis. Functional grading of the material properties along the beam height coordinate was achieved by the CNT reinforcement at different weight ratios to the layers forming the surfaces of the sandwich beams. A total of 5 different FG-CNTRC sandwich beam specimens, including a 0 wt% CNT (reference specimen) and 4 specimens which had 0.3, 0.4, and 0.5 wt% CNT and consisted of layers with different functional sequences, were produced using hand layup and vacuum diffusion methods. Three-point bending test was applied to the FG-CNTRC sandwich beams. Upon conducting both experimental and analytical research, it is possible to assert the following particular findings.

- Compared to the FGM-1 reference specimens, incorporating CNTs into the specimens resulted in benefits in their ability to withstand bending loads, with improvements that varied between −2.5% and 7.75%. The FGM-4 specimen provided the most remarkable enhancement in its load-carrying performance. The FGM-5 specimen, on the other hand, exhibited a reduction in its ability to carry loads. The amount of the CNT additive and the application level to the beam was understood to be important when comparing FGM-4 to FGM-5. Particularly, the application of 0.5 wt% additive in the outermost fiber region of the beam, such as in FGM-4, increased the bending capacity.
- When the contribution of CNT-reinforced specimens to the bending stiffness at maximum load value was compared to FGM-1, a decrease of 0.3%–18.6% was obtained. Especially, when FGM-4 and FGM-5 were examined, the stiffness loss was minimum in FGM-4, but maximum in FGM-5. This situation again pointed out that the amount of applied CNT and the location of the application are important in contributing to the stiffness.
- As a result of comparing the experimental displacements with theoretical calculations, an approximation between 11.99% and 12.98% was achieved. The experimental results were validated by formulating the Navier's solution using the high-order shear deformation theory. The actual strength of materials is several times lower than their theoretical strength. This difference is due to the natural imperfections of the material. Elimination of these defects can increase the materials' strength.
- One of the problems in the production phase is that CNT is not dispersed homogeneously in the composites. Therefore, differences may occur in the mechanical test results of the composites. There are methods suggested in the literature to overcome this situation, also known as agglomeration.
- Since the variation of shear deformations throughout the thickness of the element is expressed as high order, the condition of zero shear stresses on the lower and upper surfaces of the beams was achieved by the high order shear deformation theory, and no shear correction factor was required. When the force value taken from the experimentally obtained load-displacement curves was used within the elastic limits, theoretical and experimental results were obtained close to each other in the elastic region.

Data availability statement

The original contributions presented in the study are included in the article, further inquiries can be directed to the corresponding authors.

Author contributions

EM: Conceptualization; Methodology; Investigation; Validation; Writing–original draft. YÖ: Conceptualization; Methodology; Investigation; Validation; Writing–original draft; Writing–review and editing. AB: Conceptualization; Methodology; Investigation; Validation; Formal analysis; Resources; Writing–original draft; Writing–review and editing. IH: Conceptualization; Validation; Formal analysis. CA: Validation; Formal analysis; Writing–original draft; Writing–review and editing. MA: Methodology; Investigation; Validation. AB: Investigation; Validation; Formal analsysis; Writing–review and editing. SS: Validation; Formal analysis. ES: Investigation; Formal analysis. SF: Methodology; Validation.

Acknowledgments

The authors are thankful to the Deanship of Scientific Research at Najran University for providing support to this research work under the Research Groups Funding program grant code NU/RG/SERC/12/11 and Ministry of Science and Higher Education of the Russian Federation as part of the World-Class Research Center program, Advanced Digital Technologies (Contract No. 075-15-2022-312 dated 20.04.2022).

Conflict of interest

The authors declare that the research was conducted in the absence of any commercial or financial relationships that could be construed as a potential conflict of interest.

Publisher's note

References

Ahmad, M. N., Nadeem, S., Javed, M., Iqbal, S., Su, H., Aljazzar, S. O., et al. (2022a). Improving the thermal behavior and flame-retardant properties of poly (o-anisidine)/MMT nanocomposites incorporated with poly (o-anisidine) and clay nanofiller. *Molecules* 27, 5477. doi:10.3390/molecules27175477

Ahmad, M. N., Nadeem, S., Soltane, R., Javed, M., Iqbal, S., Kanwal, Z., et al. (2022b). Synthesis, characterization, and antibacterial potential of poly (o-anisidine)/$BaSO_4$ nanocomposites with enhanced electrical conductivity. *Processes* 10, 1878. doi:10.3390/pr10091878

Ahmad, S., Ullah, H., Rehman, Z. U., Nawaz, M., Uddin, I., Parkash, A., et al. (2022c). Investigation on crystal-structure, thermal and electrical properties of PVDF nanocomposites with cobalt oxide and functionalized multi-wall-carbon-nanotubes. *Nanomaterials* 12, 2796. doi:10.3390/nano12162796

Aksoylu, C., Özkılıç, Y. O., Madenci, E., and Safonov, A. (2022). Compressive behavior of pultruded GFRP boxes with concentric openings strengthened by different composite wrappings. *Polymers* 14, 4095. doi:10.3390/polym14194095

Allehyani, E. S., Almulaiky, Y. Q., Al-Harbi, S. A., and El-Shishtawy, R. M. (2022). In situ coating of polydopamine-AgNPs on polyester fabrics producing antibacterial and antioxidant properties. *Polymers* 14, 3794. doi:10.3390/polym14183794

Al-Muntaser, A. A., Pashameah, R. A., Sharma, K., Alzahrani, E., and Tarabiah, A. E. (2022). Reinforcement of structural, optical, electrical, and dielectric characteristics of CMC/PVA based on GNP/ZnO hybrid nanofiller: nanocomposites materials for energy-storage applications. *Int. J. Energy Res.* 46, 23984–23995. doi:10.1002/er.8695

Barretta, R., Feo, L., Luciano, R., and de Sciarra, F. M. (2015). A gradient Eringen model for functionally graded nanorods. *Compos. Struct.* 131, 1124–1131. doi:10.1016/j.compstruct.2015.06.077

Benbakhti, A., Bouiadjra, M. B., Retiel, N., and Tounsi, A. (2016). A new five unknown quasi-3D type HSDT for thermomechanical bending analysis of FGM sandwich plates. *Steel Compos. Struct.* 22, 975–999. doi:10.12989/scs.2016.22.5.975

Bisheh, H., Rabczuk, T., and Wu, N. (2020). Effects of nanotube agglomeration on wave dynamics of carbon nanotube-reinforced piezocomposite cylindrical shells. *Compos. Part B Eng.* 187, 107739. doi:10.1016/j.compositesb.2019.107739

Carrera, E., Giunta, G., and Petrolo, M. (2011). *Beam structures: classical and advanced theories*. New Jersey, United States: John Wiley and Sons.

Çelik, A., Özkılıç, Y. O., Bahrami, A., and Hakeem, I. Y. (2023). Effects of glass fiber on recycled fly ash and basalt powder based geopolymer concrete. *Case Stud. Constr. Mater.* 19, e02659. doi:10.1016/j.cscm.2023.e02659

Chakraverty, S., and Pradhan, K. K. (2016). *Vibration of functionally graded beams and plates*. Cambridge: Academic Press.

Chen, L., Zhao, Y., Jing, J., and Hou, H. (2023). Microstructural evolution in graphene nanoplatelets reinforced magnesium matrix composites fabricated through thixomolding process. *J. Alloys Compd.* 940, 168824. doi:10.1016/j.jallcom.2023.168824

Dawood, M., Taylor, E., and Rizkalla, S. (2010). Two-way bending behavior of 3-D GFRP sandwich panels with through-thickness fiber insertions. *Compos. Struct.* 92, 950–963. doi:10.1016/j.compstruct.2009.09.040

Demircan, O., Al-Darkazali, A., İnanç, İ., and Eskizeybek, V. (2020). Investigation of the effect of CNTs on the mechanical properties of LPET/glass fiber thermoplastic composites. *J. Thermoplast. Compos. Mater.* 33, 1652–1673. doi:10.1177/0892705719833105

Devi, M. K., Yaashikaa, P. R., Kumar, P. S., Manikandan, S., Oviyapriya, M., Varshika, V., et al. (2023). Recent advances in carbon-based nanomaterials for the treatment of toxic inorganic pollutants in wastewater. *New J. Chem.* doi:10.1039/D3NJ00282A

Draiche, K., Bousahla, A. A., Tounsi, A., Alwabli, A. S., Tounsi, A., and Mahmoud, S. (2019). Static analysis of laminated reinforced composite plates using a simple first-order shear deformation theory. *Comput. Concr. An Int. J.* 24, 369–378.

Draoui, A., Zidour, M., Tounsi, A., and Adim, B. (2019). Static and dynamic behavior of nanotubes-reinforced sandwich plates using (FSDT). *J. Nano Res.* 57, 117–135. Trans Tech Publ. doi:10.4028/www.scientific.net/jnanor.57.117

Elishakoff, I. E., Pentaras, D., and Gentilini, C. (2015). *Mechanics of functionally graded material structures*. Singapore: World Scientific.

Faddoul, J., Rahme, P., Guines, D., and Leotoing, L. (2023). Thermo-visco mechanical behavior of glass fiber reinforced thermoplastic composite. *J. Compos. Mater.* 57 (3), 3741–3754. doi:10.1177/00219983231192

Fayed, S., Madenci, E., Bahrami, A., Özkiliç, Y. O., and Mansour, W. (2023). Experimental study on using recycled polyethylene terephthalate and steel fibers for improving behavior of RC columns. *Case Stud. Constr. Mater.* 19, e02344. doi:10.1016/j.cscm.2023.e02344

García-Macías, E., Rodríguez-Tembleque, L., and Sáez, A. (2018). Bending and free vibration analysis of functionally graded graphene vs. carbon nanotube reinforced composite plates. *Compos. Struct.* 186, 123–138. doi:10.1016/j.compstruct.2017.11.076

Garg, A., Belarbi, M.-O., Chalak, H., and Chakrabarti, A. (2021). A review of the analysis of sandwich FGM structures. *Compos. Struct.* 258, 113427. doi:10.1016/j.compstruct.2020.113427

Gerges, N., Issa, C. A., Sleiman, E., Najjar, M., and Kattouf, A. (2023). Experimental study of the shear behavior of RC beams strengthened with high-performance fiber-reinforced concrete. *Int. J. Concr. Struct. Mater.* 17 (1), 17. doi:10.1186/s40069-023-00582-8

Gojny, F. H., Wichmann, M. H., Fiedler, B., and Schulte, K. (2005). Influence of different carbon nanotubes on the mechanical properties of epoxy matrix composites–a comparative study. *Compos. Sci. Technol.* 65, 2300–2313. doi:10.1016/j.compscitech.2005.04.021

Gul, H., Ramzan, M., Saleel, C. A., Kadry, S., and Saeed, A. M. (2023). Heat transfer analysis of a moving wedge with impact of nano-layer on nanofluid flows comprising magnetized carbon nanomaterials. *Numer. Heat Transf. A: Appl.*, 1–14. doi:10.1080/10407782.2023.2240498

Hakeem, I. Y., Özkılıç, Y. O., Bahrami, A., Aksoylu, C., Madenci, E., Asyraf, M. R. M., et al. (2024). Crashworthiness performance of filament wound GFRP composite pipes depending on winding angle and number of layers. *Case Stud. Constr. Mater.* 20, e02683. doi:10.1016/j.cscm.2023.e02683

Hellal, H., Bourada, M., Hebali, H., Bourada, F., Tounsi, A., Bousahla, A. A., et al. (2021). Dynamic and stability analysis of functionally graded material sandwich plates in hygro-thermal environment using a simple higher shear deformation theory. *J. Sandw. Struct. Mater.* 23, 814–851. doi:10.1177/1099636219845841

Huang, H., Xue, C., Zhang, W., and Guo, M. (2022). Torsion design of CFRP-CFST columns using a data-driven optimization approach. *Eng. Struct.* 251, 113479. doi:10.1016/j.engstruct.2021.113479

Hussain, M., Naeem, M. N., Tounsi, A., and Taj, M. (2019). Nonlocal effect on the vibration of armchair and zigzag SWCNTs with bending rigidity. *Adv. Nano Res.* 7, 431–442.

Jia, J., Zhao, J., Xu, G., Di, J., Yong, Z., Tao, Y., et al. (2011). A comparison of the mechanical properties of fibers spun from different carbon nanotubes. *Carbon* 49, 1333–1339. doi:10.1016/j.carbon.2010.11.054

Karam, G. N., and Tabbara, M. R. (2020). Localization and confinement efficiency in carbon fiber-reinforced plastic-confined materials. *ACI Struct. J.* 117 (6), 7–15. doi:10.14359/51728070

Kaci, A., Tounsi, A., Bakhti, K., and Adda Bedia, E. A. (2012). Nonlinear cylindrical bending of functionally graded carbon nanotube-reinforced composite plates. *An Int. J.* 12, 491–504. doi:10.12989/scs.2012.12.6.491

Li, M., Guo, Q., Chen, L., Li, L., Hou, H., and Zhao, Y. (2022). Microstructure and properties of graphene nanoplatelets reinforced AZ91D matrix composites prepared by electromagnetic stirring casting. *J. Mater. Res. Technol.* 21, 4138–4150. doi:10.1016/j.jmrt.2022.11.033

Li, S., Khan, M. I., Khan, S. U., Abdullaev, S., Mohamed, M. M. I., and Amjad, M. S. (2023). Effectiveness of melting phenomenon in two phase dusty carbon nanotubes (nanomaterials) flow of Eyring-Powell fluid: Heat transfer analysis. *Chin. J. Phys.* 86, 160–169. doi:10.1016/j.cjph.2023.09.013

Madenci, E. (2019). A refined functional and mixed formulation to static analyses of fgm beams. *Struct. Eng. Mech.* 69, 427–437.

Madenci, E. (2021). Free vibration analysis of carbon nanotube RC nanobeams with variational approaches. *Adv. Nano Res.* 11, 157–171.

Madenci, E. (2023). Fonksiyonel derecelendirilmiş malzeme plakların statik analizinde mikro-mekanik modellerin katkısı. *Necmettin Erbakan Üniversitesi Fen ve Mühendislik Bilim. Derg.* 5, 23–37.

Madenci, E., Fayed, S., Mansour, W., and Özkılıç, Y. O. (2022b). Buckling performance of pultruded glass fiber reinforced polymer profiles infilled with waste steel fiber reinforced concrete under axial compression. *Steel Compos. Struct. An Int. J.* 45, 653–663.

Madenci, E., Özkılıç, Y. O., Aksoylu, C., Asyraf, M. R. M., Syamsir, A., Supian, A. B. M., et al. (2023). Buckling analysis of CNT-reinforced polymer composite beam using experimental and analytical methods. *Materials* 16, 614. doi:10.3390/ma16020614

Madenci, E., Özkılıç, Y. O., Aksoylu, C., and Safonov, A. (2022a). The effects of eccentric web openings on the compressive performance of pultruded GFRP boxes wrapped with GFRP and CFRP sheets. *Polymers* 14, 4567. doi:10.3390/polym14214567

Mehar, K., Panda, S. K., Bui, T. Q., and Mahapatra, T. R. (2017). Nonlinear thermoelastic frequency analysis of functionally graded CNT-reinforced single/doubly curved shallow shell panels by FEM. *J. Therm. Stresses* 40, 899–916. doi:10.1080/01495739.2017.1318689

Mehar, K., Panda, S. K., Dehengia, A., and Kar, V. R. (2016). Vibration analysis of functionally graded carbon nanotube reinforced composite plate in thermal environment. *J. Sandw. Struct. Mater.* 18, 151–173. doi:10.1177/1099636215613324

Mehar, K., Panda, S. K., and Mahapatra, T. R. (2018). Nonlinear frequency responses of functionally graded carbon nanotube-reinforced sandwich curved panel under uniform temperature field. *Int. J. Appl. Mech.* 10, 1850028. doi:10.1142/s175882511850028x

Miniappan, P. K., Marimuthu, S., Kumar, S. D., Gokilakrishnan, G., Sharma, S., Li, C., et al. (2023). Mechanical, fracture-deformation, and tribology behavior of fillers-reinforced sisal fiber composites for lightweight automotive applications. *Rev. Adv. Mater. Sci.* 62 (1), 20230342. doi:10.1515/rams-2023-0342

Mirzaei, M., and Kiani, Y. (2016). Nonlinear free vibration of temperature-dependent sandwich beams with carbon nanotube-reinforced face sheets. *Acta Mech.* 227, 1869–1884. doi:10.1007/s00707-016-1593-6

Mydin, M. A. O., Jagadesh, P., Bahrami, A., Dulaimi, A., Özkılıç, Y. O., and Abdullah, M. M. A. B. (2023). Use of calcium carbonate nanoparticles in production of nano-engineered foamed concrete. *J. Mater. Res. Technol.* 26, 4405–4422. doi:10.1016/j.jmrt.2023.08.106

Özkılıç, Y. O., Gemi, L., Madenci, E., and Aksoylu, C. (2022b). Effects of stirrup spacing on shear performance of hybrid composite beams produced by pultruded GFRP profile infilled with reinforced concrete. *Archives Civ. Mech. Eng.* 23, 36. doi:10.1007/s43452-022-00576-5

Özkılıç, Y. O., Gemi, L., Madenci, E., Aksoylu, C., and Kalkan, İ. (2022a). Effect of the GFRP wrapping on the shear and bending behavior of RC beams with GFRP encasement. *Steel Compos. Struct. An Int. J.* 45, 193–204.

Pan, J., Bian, L., Zhao, H., and Zhao, Y. (2016). A new micromechanics model and effective elastic modulus of nanotube reinforced composites. *Comput. Mater. Sci.* 113, 21–26. doi:10.1016/j.commatsci.2015.11.009

Payton, E., Khubchandani, J., Thompson, A., and Price, J. H. (2017). Parents' expectations of high schools in firearm violence prevention. *J. Community Health* 42, 1118–1126. doi:10.1007/s10900-017-0360-5

Phung-Van, P., Abdel-Wahab, M., Liew, K., Bordas, S., and Nguyen-Xuan, H. (2015). Isogeometric analysis of functionally graded carbon nanotube-reinforced composite plates using higher-order shear deformation theory. *Compos. Struct.* 123, 137–149. doi:10.1016/j.compstruct.2014.12.021

Prasanthi, P. P., Kumar, M. N., Chowdary, M. S., Madhav, V. V., Saxena, K. K., Mohammed, K. A., et al. (2023). Mechanical properties of carbon fiber reinforced with carbon nanotubes and graphene filled epoxy composites: experimental and numerical investigations. *Mater. Res. Express.* 10 (2), 025308. doi:10.1088/2053-1591/acaef5

Qian, D., Wagner, A., Gregory, J., Liu, W. K., Yu, M.-F., and Ruoff, R. S. (2002). Mechanics of carbon nanotubes. *Appl. Mech. Rev.* 55, 495–533. doi:10.1115/1.1490129

Reddy, J. N. (2004). *Mechanics of laminated composite plates and shells: theory and analysis*. Boca Raton: CRC Press.

Reis, E. M., and Rizkalla, S. H. (2008). Material characteristics of 3-D FRP sandwich panels. *Constr. Build. Mater.* 22, 1009–1018. doi:10.1016/j.conbuildmat.2007.03.023

Said, Z., Rahman, S. M. A., Sohail, M. A., and Bibin, B. S. (2023a). Analysis of thermophysical properties and performance of nanorefrigerants and nanolubricant-refrigerant mixtures in refrigeration systems. *Case Stud. Therm. Eng.* 49, 103274. doi:10.1016/j.csite.2023.103274

Said, Z., Sharma, P., Bora, B. J., and Pandey, A. K. (2023b). Sonication impact on thermal conductivity of f-MWCNT nanofluids using XGboost and Gaussian process regression. *J. Taiwan Inst. Chem. Eng.* 145, 104818. doi:10.1016/j.jtice.2023.104818

Sathish, S., Prabu, D., Renita, A. A., Murugesan, K., Rajasimman, M., and Joo, S. W. (2023). Latest avenues on solar light-driven photocatalytic hydrogen generation using surface modified nanomaterials towards sustainable environment and circular bioeconomy. *Fuel* 340, 127398. doi:10.1016/j.fuel.2023.127398

Sayyad, A. S., and Ghugal, Y. M. (2019). Modeling and analysis of functionally graded sandwich beams: a review. *Mech. Adv. Mater. Struct.* 26, 1776–1795. doi:10.1080/15376494.2018.1447178

Schadler, L., Giannaris, S., and Ajayan, P. (1998). Load transfer in carbon nanotube epoxy composites. *Appl. Phys. Lett.* 73, 3842–3844. doi:10.1063/1.122911

Sehar, B., Waris, A., Gilani, S. O., Ansari, U., Mushtaq, S., Khan, N. B., et al. (2022). The impact of laminations on the mechanical strength of carbon-fiber composites for prosthetic foot fabrication. *Crystals* 12 (10), 1429. doi:10.3390/cryst12101429

Sharma, H., Kumar, A., Rana, S., Sahoo, N. G., Jamil, M., Kumar, R., et al. (2023). Critical review on advancements on the fiber-reinforced composites: role of fiber/matrix modification on the performance of the fibrous composites. *J. Mater. Res. Technol.* doi:10.1016/j.jmrt.2023.08.036

Shen, H.-S. (2009). Nonlinear bending of functionally graded carbon nanotube-reinforced composite plates in thermal environments. *Compos. Struct.* 91, 9–19. doi:10.1016/j.compstruct.2009.04.026

Su, Z., Meng, J., and Su, Y. (2023). Application of SiO_2 nanocomposite ferroelectric material in preparation of trampoline net for physical exercise. *Adv. Nano Res.* 14, 355–362.

Sun, C., Li, F., Cheng, H., and Lu, G. (2005). Axial Young's modulus prediction of single-walled carbon nanotube arrays with diameters from nanometer to meter scales. *Appl. Phys. Lett.* 87, 193101. doi:10.1063/1.2119409

Sun, L., Wang, C., Zhang, C., Yang, Z., Li, C., and Qiao, P. (2023). Experimental investigation on the bond performance of sea sand coral concrete with FRP bar reinforcement for marine environments. *Adv. Struct. Eng.* 26, 533–546. doi:10.1177/13694332221131153

Suresh, R., Gnanasekaran, L., Rajendran, S., and Soto-Moscoso, M. (2023). Doped nanomaterials: application in hydrogen production via photocatalytic water splitting. *Fuel* 348, 128528. doi:10.1016/j.fuel.2023.128528

Tabbara, M., and Karam, G. (2020). Parametric investigation of the effects of localization and slenderness on the stress–strain response and confinement efficiency in FRP-wrapped concrete cylinders. *Appl. Sci.* 10 (10), 3432. doi:10.3390/app10103432

Tarfaoui, M., Lafdi, K., and El Moumen, A. (2016). Mechanical properties of carbon nanotubes based polymer composites. *Compos. Part B Eng.* 103, 113–121. doi:10.1016/j.compositesb.2016.08.016

Thai, C. H., Ferreira, A., Rabczuk, T., and Nguyen-Xuan, H. (2018). Size-dependent analysis of FG-CNTRC microplates based on modified strain gradient elasticity theory. *Eur. J. Mechanics-A/Solids* 72, 521–538. doi:10.1016/j.euromechsol.2018.07.012

Tornabene, F., Fantuzzi, N., Bacciocchi, M., and Viola, E. (2016). Effect of agglomeration on the natural frequencies of functionally graded carbon nanotube-reinforced laminated composite doubly-curved shells. *Compos. Part B Eng.* 89, 187–218. doi:10.1016/j.compositesb.2015.11.016

Uyaner, M., and Yar, A. (2019). Nano elyaf takviyeli nanokompozit üretimi ve karakterizasyonu. *Necmettin Erbakan Üniversitesi Fen ve Mühendislik Bilim. Derg.* 1, 10–19.

Vedernikov, A., Gemi, L., Madenci, E., Özkılıç, Y. O., Yazman, Ş., Gusev, S., et al. (2022). Effects of high pulling speeds on mechanical properties and morphology of pultruded GFRP composite flat laminates. *Compos. Struct.* 301, 116216. doi:10.1016/j.compstruct.2022.116216

Vedernikov, A., Safonov, A., Tucci, F., Carlone, P., and Akhatov, I. (2020). Pultruded materials and structures: a review. *J. Compos. Mater.* 54, 4081–4117. doi:10.1177/0021998320922894

Vedernikov, A., Tucci, F., Carlone, P., Gusev, S., Konev, S., Firsov, D., et al. (2021). Effects of pulling speed on structural performance of L-shaped pultruded profiles. *Compos. Struct.* 255, 112967. doi:10.1016/j.compstruct.2020.112967

Viola, E., Rossetti, L., Fantuzzi, N., and Tornabene, F. (2014). Static analysis of functionally graded conical shells and panels using the generalized unconstrained third order theory coupled with the stress recovery. *Compos. Struct.* 112, 44–65. doi:10.1016/j.compstruct.2014.01.039

Wang, Z., Dai, L., Yao, J., Guo, T., Hrynsphan, D., Tatsiana, S., et al. (2021). Enhanced adsorption and reduction performance of nitrate by Fe–Pd–Fe3O4 embedded multi-walled carbon nanotubes. *Chemosphere* 281, 130718. doi:10.1016/j.chemosphere.2021.130718

Zhang, W., Kang, S., Liu, X., Lin, B., and Huang, Y. (2023). Experimental study of a composite beam externally bonded with a carbon fiber-reinforced plastic plate. *J. Build. Eng.* 71, 106522. doi:10.1016/j.jobe.2023.106522

Zhu, J., Peng, H., Rodriguez-Macias, F., Margrave, J. L., Khabashesku, V. N., Imam, A. M., et al. (2004). Reinforcing epoxy polymer composites through covalent integration of functionalized nanotubes. *Adv. Funct. Mater.* 14, 643–648. doi:10.1002/adfm.200305162

Zhu, P., Lei, Z., and Liew, K. M. (2012). Static and free vibration analyses of carbon nanotube-reinforced composite plates using finite element method with first order shear deformation plate theory. *Compos. Struct.* 94, 1450–1460. doi:10.1016/j.compstruct.2011.11.010